MODELING NOZZLE GEOMETRY CHANGES DUE TO THE ABLATION IN HIGH-VOLTAGE CIRCUIT BREAKERS

S. ARABI[1]*, J-Y. TRÉPANIER[1], R. CAMARERO[1] AND A. VASSILEV[2]

[1] Department of Mechanical Engineering, École Polytechnique de Montréal, Campus de l'Université de Montréal, H3T 1J4, Montréal, Canada
[2] Alstom Grid, 130 rue Léon Blum, 69611 Villeurbanne Cedex, France
sina.arabi@polymtl.ca

ABSTRACT

This paper presents a new CFD tool for transient analysis of surface ablation of a Poly-Tetra-Fluro-Ethylene (PTFE) nozzle of a high voltage circuit breaker. The developed solver fully couples the arcing flow field inside a circuit breaker chamber including radiation, ablation and nozzle wall recession. The presented numerical simulation evaluates the changes in the nozzle mass flux due to the recession of the PTFE surface, in 10 consecutive applied current cycles. During the first current cycle, the results were compared with the experimental data.

1. INTRODUCTION

Although the arcing time in the high-voltage circuit breakers is very short, it has a significant impact on the surrounding parts which are typically made of PTFE. Upon exposure to an electric arc, these parts are subjected to the severe thermal conditions inside the nozzle. The heat which radiates from the arc zone ablates and vaporizes the nozzle surface with two important effects. First, the ablated gas supplies the necessary pressure inside the pressure chambers; second, widening of the nozzle throat can affect the arc extinction procedure through a modified flow field.

Therefore, predicting the nozzle wall recession due to the ablation, and its effect on the mass flux in the nozzle, is a critical issue in the configuration design, and the operation of the device.

In this paper, a new approach is presented to evaluate the trend of the nozzle ablation and its effect on the nozzle mass flux for a long-operation time of a circuit breaker. The proposed procedure is based on a transient numerical simulation and consists in an accurate interface tracking using a mesh deformation technique coupled to the mass and energy balance at the wall.

2. FLUID EQUATIONS AND ABLATION MODEL

The Arbitrary Lagrangian Eulerian (ALE) formulation is used for solving the Euler equations of the transient compressible flow field in the nozzle. The governing equation for axisymetric flows can be written as,

$$\frac{\partial U}{\partial t} + \frac{1}{r}\frac{\partial (rF_r)}{\partial r} + \frac{\partial F_z}{\partial z} = S, \qquad (1)$$

where F_r and F_z represent the inviscid fluxes in r and z directions. In this equation two source terms for mass and energy equations have to be determined explicitly. The mass source term, S_m, results from the injection of the PTFE vapor inside the boundary cells adjacent to the nozzle wall, and is calculated at the centroid of each control volume using,

$$S_m = \frac{1}{V_p}\sum_{k=1}^{N_{sides}} \dot{m}_{p,k}, \qquad (2)$$

where V_p and N_{sides} represent the volume and number sides of each control volume, respectively. The energy source term has contributions from ohmic heating, radiated heat and ablated vapor injection,

$$S_e = S_{ohm} + S_{rad} + e_g S_m, \qquad (3)$$

where e_g is the energy per unit mass of the plasma [1]. The radiative energy is computed from the P1 approximation as follow,

$$\nabla \cdot q_{rad} = \sum_{\ell=1}^{N_{band}} \kappa_\ell (4\pi I_{b_\ell} - G_\ell), \qquad (4)$$

where q_{rad} represents the radiative flux, κ_ℓ is the mean radiation absorption coefficient averaged

over band ℓ, I_{b_ℓ} is the black-body radiation integrated over band ℓ and G_ℓ is the mean incident radiation over band ℓ as computed by the P1 model. Then, the ablated PTFE mass flux due to the radiative energy from the electric arc is,

$$\dot{m}_{p,k} = \begin{cases} \frac{\alpha q_{rad}}{h_v + \delta h_a} & \text{for an ablated side,} \\ 0 & \text{otherwise,} \end{cases} \quad (5)$$

where h_v is the vaporization enthalpy of the PTFE and δh_a is the enthalpy change in the plasma between 1000 and 3500 K. Both h_v and δh_a are assumed to be constant in the numerical modeling. The sum $h_v + \delta h_a$ represents the energy required to vaporize the PTFE and heat it to 3500 K. The parameter $0.8 \leq \alpha < 1$ represents the fraction of the heat flux which is absorbed by the PTFE's surface, the remainder being conducted deep inside the wall.

The ohmic source is computed using Joule′s heating,

$$S_{ohm} = \sigma E^2, \quad (6)$$

where $\sigma = \sigma(T, P)$ represents the electrical conductivity of the plasma. E is the electric field and can be obtained using,

$$\vec{E} = -\nabla\phi, \quad (7)$$

where the electric potential is solved using,

$$\nabla \cdot \sigma \nabla \phi = 0. \quad (8)$$

The radiative energy source term is,

$$S_{rad} = \nabla \cdot q_{rad}. \quad (9)$$

The absorbed energy causes the wall temperature to reach the vaporization temperature which is nearly $T \geq 1000$. The effect of this vaporization is modeled by injecting a mass flux, Eq. 5, to the boundary cells through the corresponding edges adjacent to PTFE wall. Based on the calculated mass flux and PTFE's density (ρ), the wall recession velocity in the direction normal to the boundary edges can be obtained easily by Eq. 10.

$$\vec{V}_{edge} = \frac{\dot{m}_{p,k}}{\rho S_k}, \quad (10)$$

where, S_k is the area of the boundary side k of the cell p. In practice, because the distances between the boundary edges from the arcing region are different, they receive different heat, and, consequently different injected mass inside their adjacent cells. Hence, according to Eq. 10, the edge velocities vary along the nozzle wall. Therefore, recessing the nozzle wall based on the edge velocities generates invalid cells and results in a configuration shown in Fig. 1.

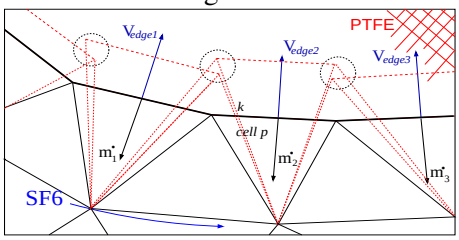

Fig. 1: *Invalid cells resulting from moving the ablated wall based on the edges velocity. The dashed lines represent the recessed boundary edges.*

Hence, to avoid any discontinuity in the boundary motion, the wall is recessed based on the node velocities. On the PTFE surface, the node velocities are computed by averaging the velocities of its neighboring edges,

$$\vec{V}_{node_i} = \left[\left(\vec{V}_{edge}\right)_{Left} + \left(\vec{V}_{edge}\right)_{Right}\right]/2 \quad (11)$$

Figure 2 illustrates schematically the injected mass flux to the boundary cells and the node velocities which are obtained by the edge velocities.

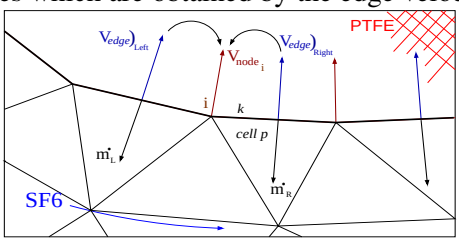

Fig. 2: *Converting the mass flow rate to the boundary velocity and nodal velocity.*

By having $\vec{V}_{node_i}$ due to the nodal ablation rate, the nodal velocities on the interior mesh nodes can be determined simply by solving a Laplace equation. Then, the obtained nodal velocities are used in ALE solver to compute the fluxes passing through the moving cell sides, and also updating the position of the mesh nodes respectively.

3. PROBLEM DEFINITION

The numerical model described in the previous section is applied to the configuration shown in Fig. 3. This geometry represents a real circuit-breaker chamber and has been extensively studied by [2] and for which there are pressure measurements in four different locations in [3]. An upstream total pressure of 7.48 atm is imposed

at the inlet, and the exit static pressure is 1 atm. The arc is stabilized between the electrode tips on the axis by SF_6 gas blowing from inlet (left) to outlet (right of the Fig. 3). The first step in this study was to compare the numerical simulation for cold flow with the experimental data [3] at the sites shown in Fig. 3. Then, the flow in arcing mode is evaluated and compared with the experimental results. Finally, to study the ablation effects on the mass flow rate, the current shown in Fig. 4 is imposed to the configuration. The applied current cycle is repeated in 10 consecutive times to predict the changes in the nozzle mass flux in a long-operation time. In the present simulation, the peak current is 56kA and the arcing time for each cycle is 6.4ms. The first 6ms with 1kA current is just considered for initialization of the flow field inside the nozzle.

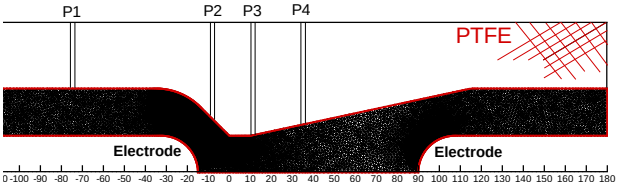

Fig. 3: *Generated mesh, electrodes and positions of the pressure sensors.*

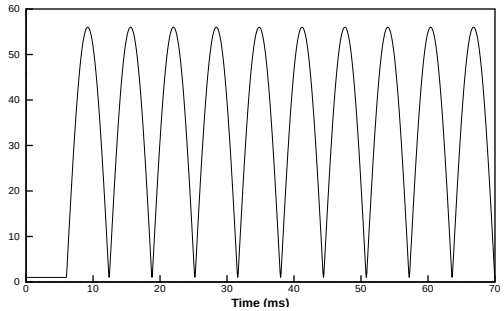

Fig. 4: *Imposed current variation for 10 operational cycle for a peak current of 56k.*

4. RESULTS AND DISCUSSION

Figure 5 shows a high accuracy numerical result of axial pressure distribution on the upper side of the nozzle.

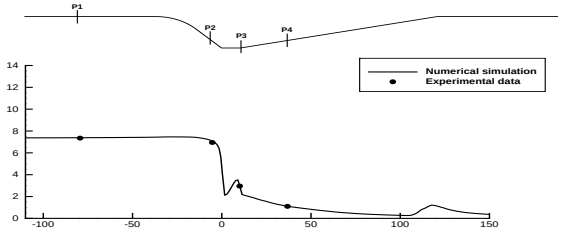

Fig. 5: *Axial pressure distribution for the cold flow condition.*

The next step is applying the current variation to the cold flow. The resulting pressure distribution for the arcing flow at three different times are shown in Figs. 6-8 and during the first current cycle of Fig. 4.

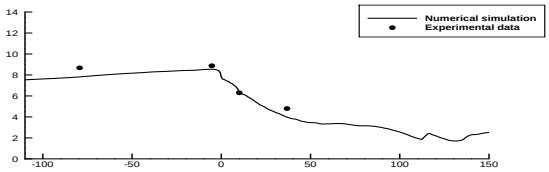

Fig. 6: *Axial pressure distribution at, t=7ms, I=26.4 kA.*

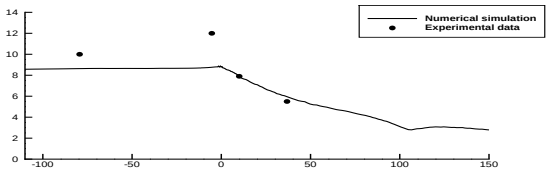

Fig. 7: *Axial pressure distribution at, t=9ms, I=55.7 kA.*

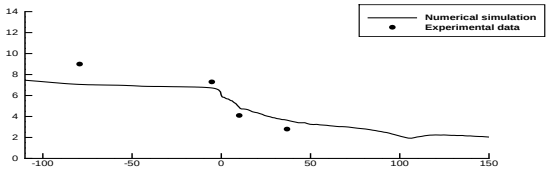

Fig. 8: *Axial pressure distribution at, t=11ms, I=35.5 kA.*

As can be seen from Figs. 6-8, the pressure has been increased by applying the current, and reaches its maximum around the peak current. It is quite apparent that this effect is due to the forming and growing of an obstruction and consequently reducing of the effective nozzle area. The major reason of the obstruction in the arcing flow is shown in Fig. 9. According to the imposed current to the flow field, the temperature rises dramatically which is accompanied by a steep fall in density inside the arc region. Hence, the arc region behaves like a impermeable obstacle obstructing the flow field.

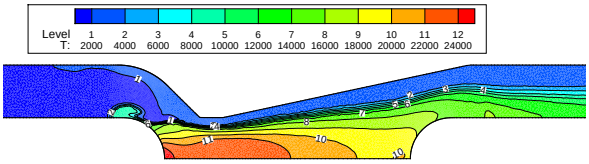

Fig. 9: *Temperature field at the peak current.*

At the peak current, radiation by the arc is mostly absorbed by the nozzle wall, the thermal region is raised and the injected gas into the domain as a result of ablation reaches a maximum. The combined effect is a clogging of the flow in the chamber and a rise in pressure, specially around

the P2 site as shown in Fig. 7. As a consequence, the direction of the flow reverses, and the gas exhausts from both sides of the nozzle as can be seen by the flow field shown in Fig. 10.

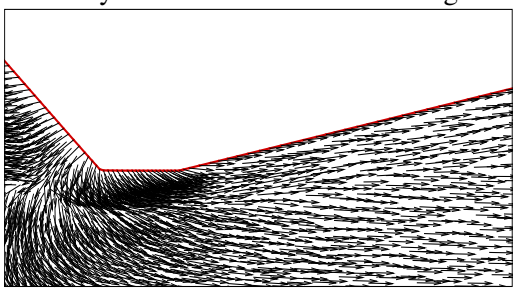

Fig. 10: *Non-scaled velocity vector field at the peak current.*

Figure 11 shows the scaled recession velocity of the wall near the peak current. As can be seen by this figure, the maximum deformation, or mass loss, is located at the nozzle throat, as observed in commercial circuit-breakers in practice.

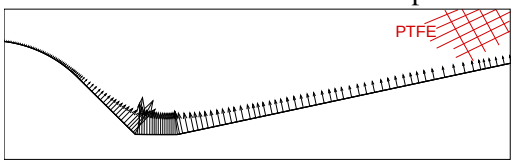

Fig. 11: *Nodal velocities due to the ablation on the upper wall of the nozzle at, t=9ms, I=55.7 kA.*

To gain more insight into the rate of ablation, the simulation has been carried out for 10 consecutive current cycles. To evaluate the effect of the wall deformation on the circuit-breakers performance, the mass flux at the throat and at the end of each current cycle is studied. Figure 12 shows how the nozzle throat widens after 10 current cycle which is about 6.5% of the original radius. It is apparent that the nozzle wall moves gradually in pace with the imposed current law.

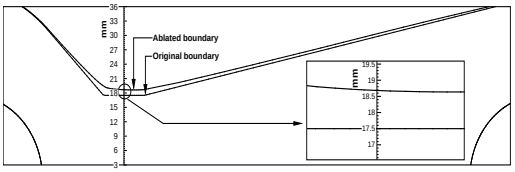

Fig. 12: *Geometry change after applying 10 current cycle.*

As it can be seen from Fig. 13, despite the small fluctuations, the global trend of the mass flow rate passing through the throat increases. This graph is presented without the initialization time of the fluid flow inside the nozzle. By comparing the amounts between the end of the 10^{th} and 1^{st} cycles, there is about a 9.5% rise in the mass flow rate.

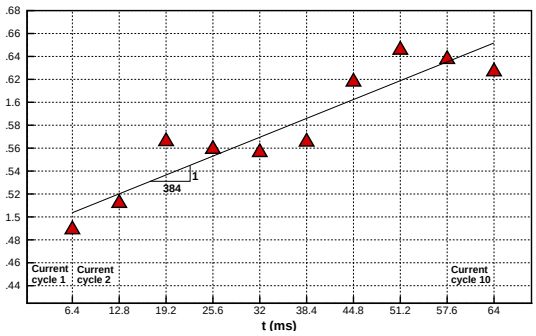

Fig. 13: *Variation in the mass flow rate for 10 applied current cycle.*

5. CONCLUSION

A new transient ablation model was performed through simulation of a PTFE nozzle of a circuit breaker in a long-operation time. The radiated heat from the electric arc recessed the nozzle surface, widened the throat and consequently, raised the mass flux. The pressure variation for both cold and arcing flow on the nozzle surface were computed, and reasonable agreement with the experimental data was achieved. Only near the peak current, and at the P1 and P2 sites, did the presented numerical solution demonstrate the need for a more accurate radiation model. However, the proposed model clearly showed the clogging of the nozzle and the ablated gas dominant flow field near the peak current. The mass flux was calculated at the throat and at the end of each current cycle. This study has demonstrated its ability to simulate qualitatively and to some degree, quantitatively the ablated effect under operating conditions. It is expected that this model can be used as a promising tool for designers to predict the effectiveness of the arc extinction mechanism in the circuit breakers and in its life time.

REFERENCES

[1] D. Godin, J-Y. Trépanier, M. Reggio, X.D. Zhang and R. Camarero, "Modelling and simulation of nozzle ablation in high-voltage circuit-breakers" J. Phys. D: Appl. Phys. **33**, 2583–2590, 2000.

[2] E. Lewis, "The thermal properties of an SF_6 circuit breaker arc during the current zero period" PhD Thesis University of Liverpool, 1987.

[3] S. Taylor, M.T.C. Fang, G.R. Jones and D.W. Shimmin, "Current zero flow conditions in a circuit breaker-nozzle" Science, Measurement and Technology, IEE Proceedings A **138-5** 259–264, 1991.